JOURNAL OF Materials CHEMISTRY

Modelling the interfaces between calcite crystals and Langmuir monolayers

Dorothy M. Duffy* and John H. Harding

Department of Physics and Astronomy, University College London, Gower Street, London, UK WC1E 6BT. E-mail: d.duffy@ucl.ac.uk

Received 12th June 2002, Accepted 9th August 2002
First published as an Advance Article on the web 11th September 2002

Langmuir monolayers are good model systems for investigating the use of organic templates to control the growth and morphology of calcium carbonate. We investigate the structure of the organic–mineral interface using molecular dynamics methods. The monolayer consists of octadecanoic (stearic) acid molecules; the calcium carbonate is the calcite phase. Seven interfaces were chosen to demonstrate the various types of behaviour possible. We show that simple epitaxial arguments based on the ideal, unrelaxed monolayer and mineral surfaces can be very misleading, particularly when considering polar directions. Furthermore, such arguments cannot predict the relative stability of the various interfaces. We show that the polar (001) direction (with a Ca termination) produces the most stable interface and discuss the implications for mineral growth on organic monolayers.

Introduction

The ability of organisms to grow complex organic–inorganic composite materials with exceptional structural properties has attracted considerable interest in recent years. The possibility of mimicking these processes to design new composite materials with a desired set of properties has generated significant research effort into the control of inorganic crystal growth with organic molecules.[1] The study of calcium carbonate is of particular interest because of the major role it plays in biomineralization and because of the range of stable morphologies and crystalline forms it exhibits.

The growth of calcium carbonate crystals on a range of organic molecules and templates has been studied extensively experimentally. Langmuir monolayers,[2] self-assembled monolayers[3,4] and polymers[5–7] have all been used as substrates for calcium carbonate crystal growth. The chemical composition and the surface pressure of the substrate, as well as the acidity of the growth solution, have been found to have a strong influence on the resulting crystal morphologies. It would appear that steric matching has a role to play in favouring a particular growth face, but the details of how the structure of the substrate influences nucleation is poorly understood.

In order to gain insight into the interaction between Langmuir monolayers and calcium carbonate surfaces, we have modelled interfaces using molecular dynamics techniques. We present the results of a study of the interfaces between monolayers of octadecanoic acid (stearic acid) and the low energy faces of calcite. Octadecanoic acid is a typical example of a long chain carboxylic acid that forms a Langmuir monolayer on the surface of water. The monolayer exhibits a rich phase behaviour with varying surface pressure and temperature, with a solid-like phase at high surface pressure, a gas-like phase at low surface pressure and a number of liquid-like phases at intermediate pressures, with different degrees of tilting of the hydrocarbon tails. The controllability of the surface densities of Langmuir monolayers make them ideal substrates for the study of inorganic crystal growth at organic surfaces.

Simulated interfaces were formed by relaxing octadecanoic acid monolayers, with surface densities commensurate with the crystal surface structure, onto the calcite surface. The resulting configurations were examined for a range of surfaces at three temperatures and the interfacial energies were calculated. The structure of the hydrogen bonding between the acid head groups of the monolayer and the crystal surface was studied for each interface. The implications of the results for calcite crystal growth on octadecanoic acid monolayers are discussed.

Method and procedures

The molecular dynamics program DL_POLY[8] was used to calculate structures and energies in this project. The interactions between the atoms of the organic molecules were modelled using a combination of two force-field parameter sets. The CHARMM22 force field parameters[9] were used for the interactions between the atoms of the head groups and the tails were modelled using the united atom model of Kim *et al.*[10] The calcite crystal was modelled using the shell model parameters derived by Pavese *et al.*,[11] previously used successfully to calculate surface energies of calcium carbonate crystals.[12] The charges of the head group atoms were those associated with the CHARMM22 force field. The non-bonded interactions between the crystal surface and the monolayer are derived from the CHARMM22 interactions for the Ca^{2+} and CO_3^{2-} ions and the head group atoms using the usual Lorentz mixing rules. A cut-off of 10.1 Å was used for the non-bonded interactions.

The correct treatment of electrostatics is essential in this kind of problem. Interfaces retain only two-dimensional periodicity. It is possible to perform electrostatic summations in two dimensions.[13] The METADISE code,[14] which performs a static lattice minimisation on interfaces between two semi-infinite blocks of crystal, uses this approach. It is more usual to use conventional 3-D Ewald summations and three-dimensional periodicity. This was done here, with a vacuum gap of at least 50 Å between the two-dimensional slabs. An Ewald parameter (α) of 0.32 and reciprocal space vectors $k_x = k_y = 9$, $k_z = 23$ were used to ensure satisfactory convergence of the Ewald sum. However, there is a well-known problem arising from the conditional convergence of the Coulomb summation for certain interfaces. The normals to these interfaces, the *polar directions*, define a stack of charged planes with a macroscopic dipole. In such cases, the energy to form the interface diverges. This is not merely a theoretical quibble; real surfaces that are

defined by polar directions undergo gross reconstructions to remove the dipole. Typically, they either facet or become highly defective. To perform meaningful calculations on such interfaces, it is necessary to quench the dipole. This is done by moving charge from the topmost plane of the stack to form a new plane at the bottom. In simple cases, as here, a half-plane of charge is moved from top to bottom, producing two identical defective surfaces. In general,[15] more complex transfers are required. Polar directions are important in growing crystals with divalent cations on Langmuir monolayers because the ionised monolayer gives a natural half-plane to quench the dipole.

Five calcite surfaces were considered in this study. Three of these, the (104), (110) and (100) surfaces, have equal numbers of Ca^{2+} and CO_3^{2-} ions and, hence, a unique termination. The crystallographic directions of the other two faces studied [the (001) and the (012) surfaces] have alternating layers of Ca^{2+} and CO_3^{2-} ions, therefore they can be terminated either with a plane of Ca^{2+} ions or a plane of CO_3^{2-} ions. The dipoles for these directions were quenched in the manner discussed above. The (104), (110), (100) and (001) surfaces have been previously modelled by Parker and de Leeuw[12] using static relaxation techniques. We have chosen to include the (012) surface in the simulation set because Berman and Charych[7] have found a strong tendency for (012) calcite nucleation on polymeric long chain acid monolayers.

The calcite surfaces were modelled by forming two-dimensional slabs approximately 16 Å thick in the required crystallographic orientation. The thickness of the slab varies between surfaces due to the different interplanar spacing. The size and shape of the simulation cells for each interface are summarized in Table 1, together with the total number of surface unit cells in the simulation cell.

The structure of the monolayer for each interface was chosen such that the surface unit cell matched the calcite surface. The number of molecules in the unit cell was chosen to give a surface area per molecule between 19 and 25 $Å^2$ in order to match the experimental surface areas of compressed monolayers of carboxylic acids. This is within the compressed liquid range of the monolayer and within the regime used in the experiments (ref. 2 and B. Heywood, private communication). The total number of octadecanoic acid molecules in each simulation cell is also included in Table 1. We note that, in order to obtain a density in the required range, the monolayer surface cell is incommensurate with the crystal surface for the (012) interface. There are, in fact, three monolayer cells for every two crystal surface cells.

The simulations were performed using the general purpose molecular dynamics program DL_POLY. The interface was constructed from an initial configuration in which a 2-dimensional array of octadecanoic acid molecules was placed 4 Å above an unrelaxed calcite surface. The unrelaxed surface was formed by cutting the bulk crystal along the required crystallographic orientation and, in the case of the dipolar surface, moving half of the ions from the top surface of the slab to the bottom. The monolayer was relaxed onto the frozen crystal surface during a 100 ps simulation (timestep 1 fs) at 10 K. A Nosé-Hoover thermostat with a relaxation time of 0.01 ps was used to maintain a constant temperature. The initial configuration of the monolayer had the alkane chains arranged in a herring-bone configuration, with alternating orientations of the cross-section of the chains. The herring-bone configuration is generally the lowest energy conformation for molecules with long alkane chains.[16] Several distinct lateral displacements were chosen as starting configurations for each simulation and the final configuration with the lowest energy was chosen for the subsequent simulations. Clearly, there are an infinite number of possible starting configurations for such complex systems and we cannot hope to explore all of phase space. Nevertheless, we should have at least identified a deep local minimum for each interface. A 10 K, 100 ps simulation (timestep 1 fs) of the isolated monolayer was performed to obtain a reference state for the monolayer.

The final configurations from the 10 K simulations were used as initial configurations for a further set of simulations, from which the relaxed energies and structures of the interfaces were determined. In these simulations, the octadecanoic acid molecules and the atoms in the top half of the crystal slab were mobile and the bottom half of the slab was frozen. In cases with an odd number of crystal layers, the extra layer was frozen. It was necessary to use a reduced timestep of 0.1 fs because of the very small mass of the O shell (0.2 amu). Simulations of 10 ps were carried out at 2, 100 and 300 K, and the energy at each temperature, averaged over the final 8 ps to allow for equilibration, was calculated. Equivalent simulations were carried out for the isolated calcite surfaces and for the isolated monolayer. The final configurations from the 10 K simulations were used as initial configurations for the monolayer simulations. The interfacial energy was determined from the difference between the energy of the interface and the sum of the energies of the isolated surface and the monolayer.

The hydrogen bonding between the hydrogen atoms of the monolayer and the oxygen atoms of the crystal surface was studied for each interface and compared with the hydrogen bonding between the acid head groups of the isolated monolayers. We have chosen a maximum hydrogen bond length of 2.2 Å and calculated the average number of such bonds over the final 8 ps of each simulation.

Results and discussion

A common measure of the strength of an interface is the *interfacial binding* energy. This is the energy cost of cleaving the interface to create two surfaces. This can be written as

$$\Gamma_I = [E\,(\text{block containing interface}) - E\,(\text{X half-block including surface}) - E\,(\text{Y half-block including surface})]/A \quad (1)$$

where A is the area of the interface, as before. Γ_I should be negative; it costs energy to break a stable interface. In effect, it is the adhesion energy for the film to bind to the mineral. The calculated interfacial binding energies are summarised in Table 2. It is important to note that these energies are with respect to a vacuum. The experimental systems are, of course, prepared in water. Preliminary calculations on hydrated systems suggest that, although the absolute energies are different, the relative ordering is still a good measure of the strength of

Table 1 The size and shape of the simulation cells for each surface

Surface	Type	Thickness/Å	Surface unit cell				No. of cells in simulation	No. of $C_{17}COOH$
			Shape	a/Å	b/Å	γ/°		
(104)	Neutral	18.1	Rectangular	4.79	8.04	90	35	70
(110)	Neutral	14.4	Rhomboidal	6.45	11.98	141	35	70
(100)	Neutral	17.3	Rectangular	4.79	17.48	90	21	84
(001)	Dipolar	14.7	Hexagonal	4.79	4.79	120	36	36
(012)	Dipolar	18.8	Rectangular	4.79	6.45	90	28	42

Table 2 Interfacial energies and surface energies for the calcite–octadecanoic acid monolayer interfaces

Surface	Surface energy/J m^{-2}	Interfacial energy/J m^{-2}		
		2 K	100 K	300 K
(104)	0.60	−0.92	−0.92	−0.81
(110)	1.43	−0.84	−0.84	−0.88
(100)	0.95	−0.92	−1.04	−1.11
(001) Ca	0.97	−1.00	−1.06	−1.12
(001) CO_3	0.99	−0.89	−0.90	−0.93
(012) Ca	1.25	−0.78	−0.85	−0.92
(012) CO_3	1.06	−0.72	−0.76	−0.83

Table 3 The energy per molecule of the isolated monolayers

Surface	Monolayer energy per $C_{17}H_{35}COOH$/kJ mol^{-1}			Area per $C_{17}H_{35}COOH$ molecule/$Å^2$
	2 K	100 K	300 K	
(104)	−194.4	−174.6	−126.7	19.3
(110)	−188.3	−152.9	−113.0	24.2
(100)	−183.3	−165.6	−119.2	21.0
(001)	−192.6	−173.3	−125.4	19.9
(012)	−190.2	−170.4	−125.4	20.6

the interfacial adhesion.The relaxed surface energies, calculated using the static relaxation program METADISE,[14] are also included in the table for comparison. (Surface energies, σ, are usually defined as the energy required to cleave a block, hence,

$$\sigma = [E\text{ (separated blocks after breaking)} - E\text{ (block before breaking)}]/2A \quad (2)$$

where A is the area of the interface and the factor of 2 is because two surfaces are created). These energies have previously been discussed in detail in ref. 12.

The magnitude of the interfacial binding energy is high for each interface, comparable to the typical value for the surface energy. The magnitude of the interfacial energy tends to increase with temperature primarily because increasing the temperature increases the disorder of the isolated monolayer more than that of the attached monolayer. The energies per molecule of the isolated monolayer at the three calculation temperatures are summarised in Table 3. The energies of the monolayer have no independent significance; they are reported here to show the origin of the temperature dependence of the interfacial binding energy. The interfacial binding energies reported here are a measure of the adhesion of the various calcite surfaces to the organic film. These show that some polar surfaces of calcite are bound as strongly to the film as the (104) surface, which dominates the morphology of calcite under normal growth conditions. This suggests how the presence of such films can encourage the growth of unusual morphologies in biological systems.

The mean numbers of hydrogen bonds per octadecanoic acid molecule, calculated from the final 8 ps of each simulation, are summarised in Table 4. Three series of results are recorded, the number of hydrogen bonds between the H atoms of the monolayer and the O atoms of the crystal surface, the number of hydrogen bonds between the monolayer molecules on the surface and the number of hydrogen bonds in the isolated monolayer. In the isolated monolayer, there are between 0.5 and 0.8 hydrogen bonds per molecule, with the lowest density of hydrogen bonds corresponding to the low density monolayer for the (110) interface. When the monolayers are on the crystal surface, the intra-monolayer hydrogen bonding is reduced significantly, in fact, it is negligible for all cases except the (012) Ca-terminated interface. The hydrogen bonding between the monolayer and the crystal surfaces is substantial, with most interfaces having at least one bond per monolayer molecule. The (012) Ca-terminated interface is again an exception, with only two thirds of the monolayer molecules bonding to the surface in the low temperature simulation. A visual inspection of the final configuration shows that one third of the rows of surface molecules experience intra-monolayer hydrogen bonding and are not bonded to the surface.

The atomic structures of the surfaces and interfaces were captured at the end of the simulation period and these are presented for the 2 K simulations of four of the interfaces in Fig. 1–8. The side views of the interface, surface and monolayer (Fig. 1–4) show the modification of the surface structure by the adsorbed monolayer and the modification of the monolayer configuration by adsorption on the surface. The top views of the isolated monolayer and the monolayer on the crystal surface (Fig. 5–8) emphasise the different tilt directions for the two cases.

The results suggest that the interfacial structures can be divided into two broad classes; those with surface structure largely unchanged by the adsorbed monolayer and those where the monolayer causes significant modification. The (104) interface (Fig. 1) is an example of the former. The {104} faces dominate the morphology of calcite crystals grown from pure solution and calculations find the (104) surface to have the lowest energy, both in a vacuum and in an aqueous environment.[12] There is little relaxation from the bulk configuration, either in the free surface [Fig. 1(c)] or in the interface with the monolayer [Fig. 1(a)]. The adsorbed monolayer is ordered, with the OH groups forming hydrogen bonds with the surface carbonate ions and the carbonyl O directed towards the Ca ions.

The (100) interface (Fig. 2) is an example of a case where the adsorbed monolayer modifies the surface structure significantly. The bulk termination of this orientation has the plane of the carbonate ions lying perpendicular to the surface, and earlier simulations[12] have demonstrated that such a perpendicular configuration is unfavourable. There is, therefore, significant rotation on relaxation of the surface ions [Fig. 2(b)]. The adsorption of the monolayer [Fig. 2(a)] reduces this rotation. The monolayer fits well into the corrugations of

Table 4 Monolayer–crystal and intra-monolayer hydrogen bonds

Surface	Hydrogen bonds per $C_{17}H_{35}COOH$ molecule								
	Calcite–monolayer			Intra-monolayer			Isolated monolayer		
	2 K	100 K	300 K	2 K	100 K	300 K	2 K	100 K	300 K
(104)	1.12	1.11	1.01	0.00	0.00	0.00	0.68	0.82	0.80
(110)	1.37	1.41	1.18	0.00	0.00	0.00	0.56	0.56	0.62
(100)	0.94	1.18	1.21	0.01	0.00	0.00	0.77	0.74	0.69
(001) Ca	0.92	0.96	0.99	0.00	0.00	0.00	0.78	0.77	0.62
(001) CO_3	1.00	1.00	0.88	0.00	0.00	0.12			
(012) Ca	0.67	0.71	0.82	0.14	0.14	0.12	0.75	0.72	0.63
(012) CO_3	1.02	0.92	0.90	0.05	0.08	0.11			

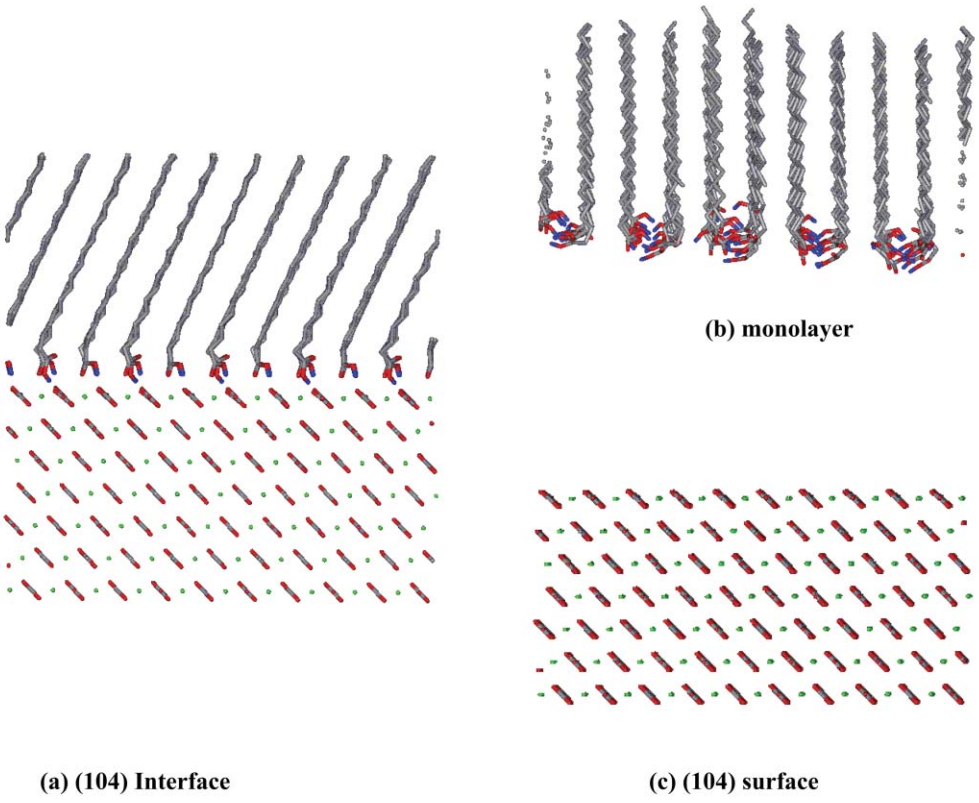

Fig. 1 Side view of the final configuration for the 2 K 10 ps simulations of (a) the (104) surface–monolayer interface, (b) the isolated octadecanoic acid monolayer (19.3 $Å^2$ $molecule^{-1}$) and (c) the (104) calcite surface.

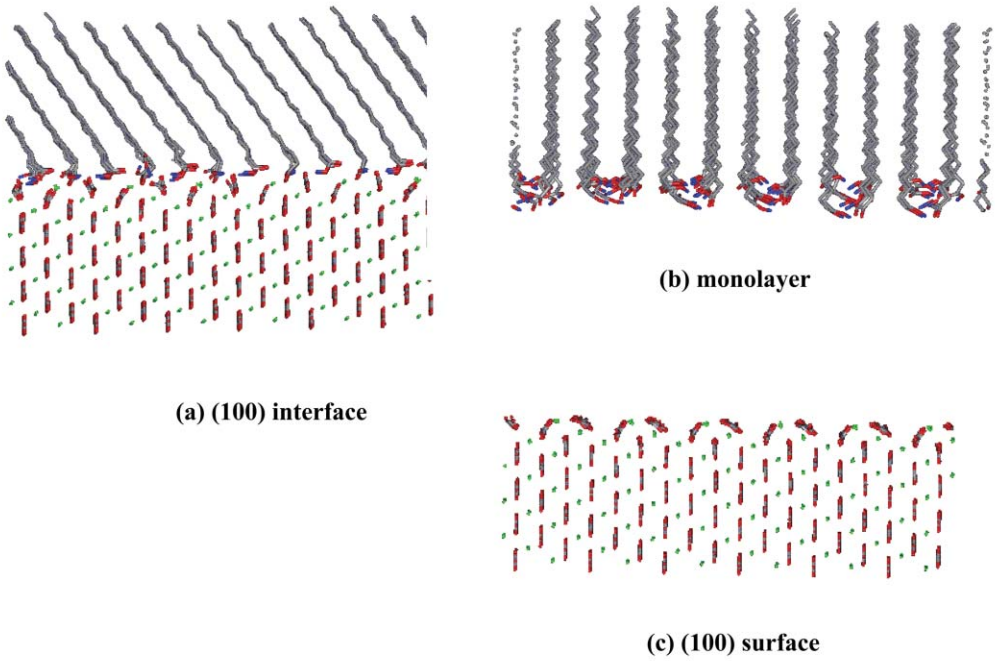

Fig. 2 Side view of the final configuration for the 2 K 10 ps simulations of (a) the (100) surface–monolayer interface, (b) the isolated octadecanoic acid monolayer (21.0 $Å^2$ $molecule^{-1}$) and (c) the (100) calcite surface.

this surface and, again, a high density of hydrogen bonds is formed between the monolayer and the surface.

The monolayer has also a significant effect on the (110) surface. It tends to reduce the surface relaxation, resulting in a structure that closely resembles the bulk termination.

The (001) polar interface is shown for both CO_3 (Fig. 3) and Ca termination (Fig. 4). The CO_3-terminated surface has a very similar structure with and without the adsorbed monolayer. The monolayer head groups are adsorbed into the gaps left by the missing carbonate ions and the adsorbed monolayer is strongly ordered. There is significant reconstruction of the Ca-terminated surface by the adsorbed monolayer. The free surface relaxes to form microfacets, with the carbonate groups rotating from the as-cut orientation parallel to the surface

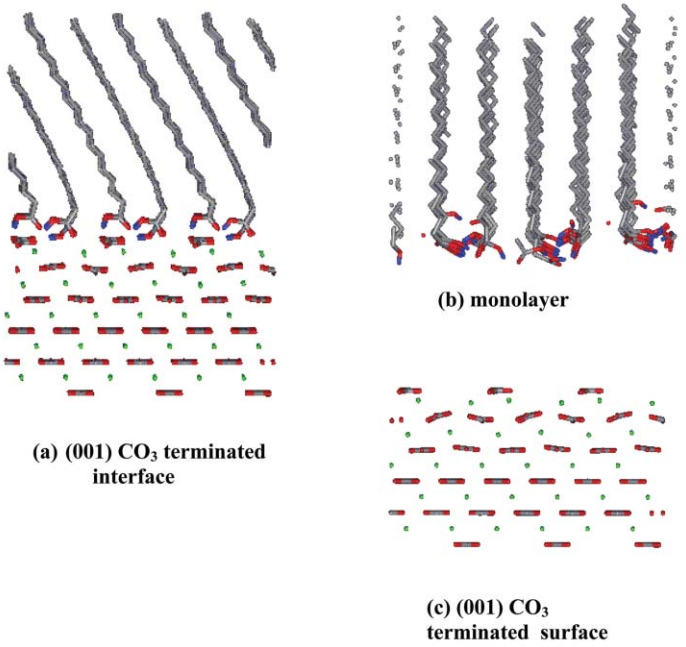

Fig. 3 Side view of the final configuration for the 2 K 10 ps simulations of (a) the (001) CO_3-terminated surface–monolayer interface, (b) the isolated octadecanoic acid monolayer (19.9 $Å^2$ $molecule^{-1}$) and (c) the (100) CO_3-terminated calcite surface.

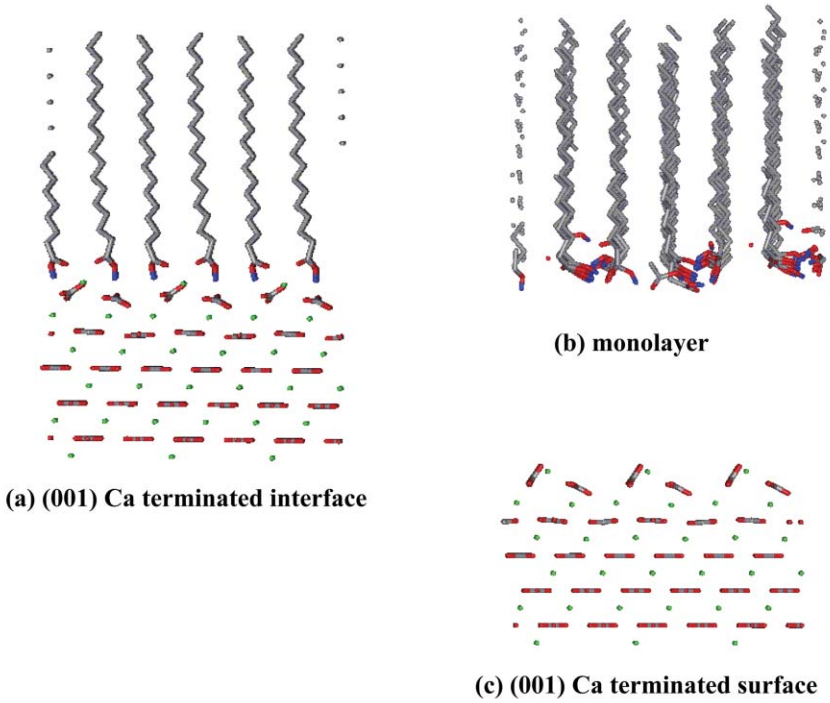

Fig. 4 Side view of the final configuration for the 2 K 10 ps simulations of (a) the (001) Ca-terminated surface–monolayer interface and (b) the (001) Ca-terminated calcite surface.

[Fig. 4(c)]. The rotation is reduced by the monolayer, which again adopts a highly ordered conformation and forms a high density of hydrogen bonds with the surface [Fig. 4(a)].

The second polar interface modelled [the (012) interface] is, in some respects, the opposite of the (001) interface because here it is the CO_3 interface that is strongly affected by the adsorbed monolayer, whereas the structure of the Ca-terminated surface is largely unchanged. Unlike all the other cases considered, where the inter-monolayer hydrogen bonding is negligible at the interface, there is some residual inter-monolayer hydrogen bonding for the (012) interface. The monolayer–surface hydrogen bonding is relatively low for the (012) Ca-terminated surface.

It is also interesting to note the effect of adsorption on the configuration of the monolayer. The tilt directions of the monolayer tails were examined by calculating the direction of the principal axis corresponding to the smallest eigenvalue of the moment of inertia tensor of the alkane chain. The angles between the principal axis and the surface normal (θ) and the azimuthal angles (ϕ) between the projection of the principal axis onto the surface plane and the y-axis were calculated for each tail at 0.1 ps intervals during the 2 K simulation. The mean values, averaged over the monolayer and over the simulation period, are summarized in Table 5.

The angle of tilt to the normal correlates with the density of the monolayer as it is primarily determined by packing

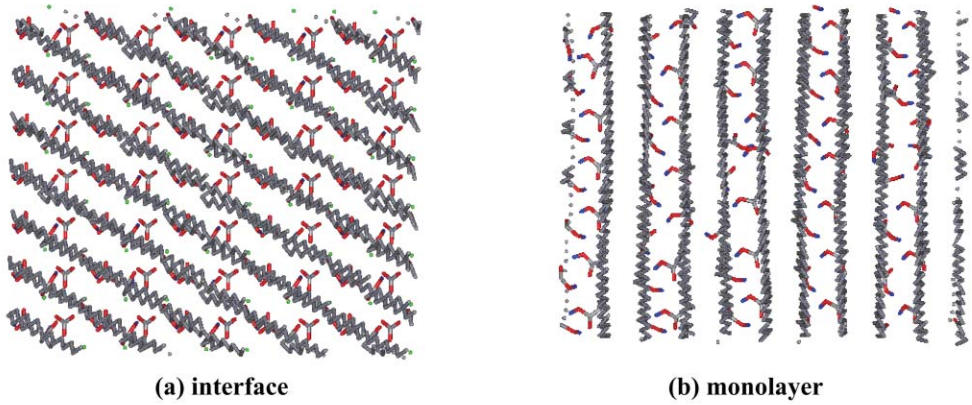

Fig. 5 Top view of the final configuration for the 2 K 10 ps simulations of (a) the (104) surface–monolayer interface and (b) the isolated octadecanoic acid monolayer (19.3 $Å^2$ $molecule^{-1}$).

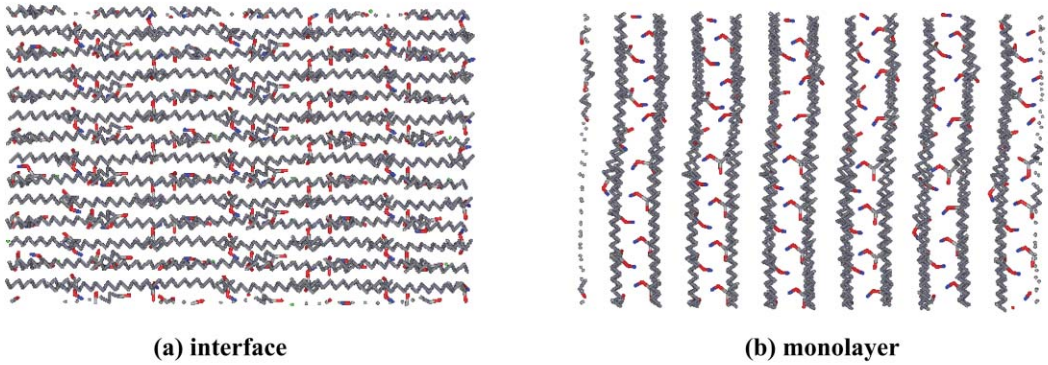

Fig. 6 Top view of the final configuration for the 2 K 10 ps simulations of (a) the (100) surface–monolayer interface and (b) the isolated octadecanoic acid monolayer (21.0 $Å^2$ $molecule^{-1}$).

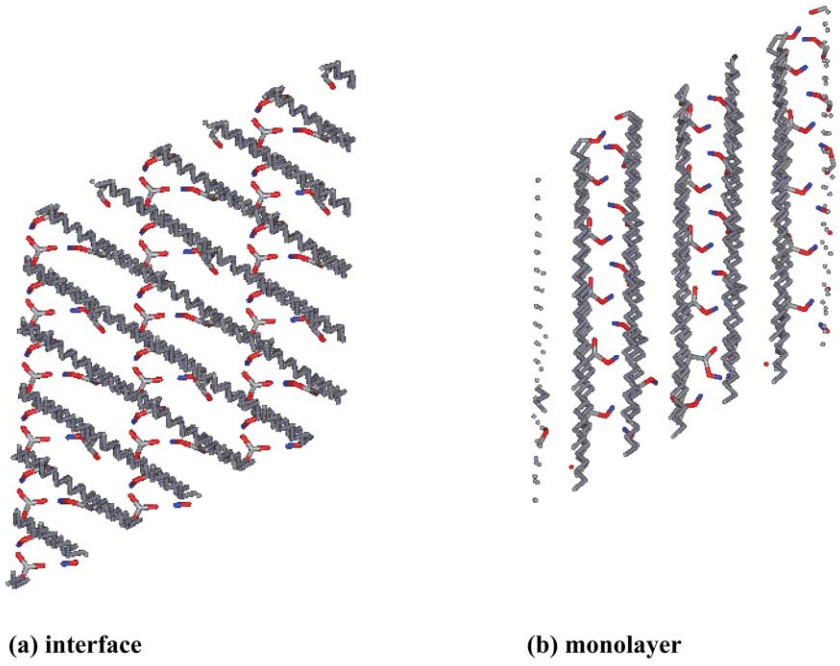

Fig. 7 Top view of the final configuration for the 2 K 10 ps simulations of (a) the (001) Ca-terminated surface–monolayer interface and (b) the isolated octadecanoic acid monolayer (19.9 $Å^2$ $molecule^{-1}$).

constraints. Adsorption of the monolayer has little effect on this angle. An exception is the (110) interface that has a low density monolayer which is rather disordered, both on the surface and in free space. Adsorption has a more significant effect on the azimuthal angle. Nearest neighbour and next nearest neighbour tilt directions are seen in different phases of Langmuir monolayers. We found that adsorption onto the surface expedited a shift from one tilt direction to another, with the 3rd neighbour tilt direction being favoured on some surfaces.

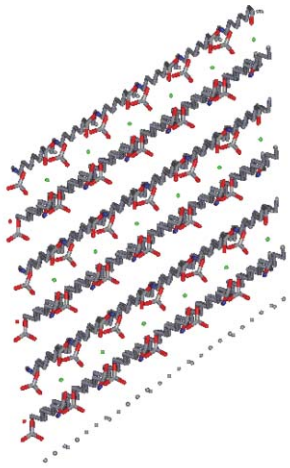

Fig. 8 Top view of the final configuration for the 2 K 10 ps simulations of the (001) CO_3-terminated surface–monolayer interface.

Table 5 The angle to the normal (θ) and the azimuthal angle (ϕ) of the monolayer tails on the surface and in the isolated monolayer

	Monolayer on surface			Isolated monolayer		
Surface	θ	ϕ	Tilt direction	θ	ϕ	Tilt direction
(104)	26.1	70.2	nn	26.6	8.4	nnn
(110)	36.2	63.6	nn	44.7	1.4	nnn
(100)	33.8	87.8	3rd nn	31.9	3.4	nn
(001) Ca	30.3	63.6	nn	29.7	2.3	nn
(001) CO_3	28.3	56.8	nn			
(012) Ca	31.8	4.5	3rd nn	33.1	25.1	nnn
(012) CO_3	30.6	7.2	3rd nn			

[a]nn Refers to nearest neighbour tilt, nnn to next nearest neighbour tilt and 3rd nn to third nearest neighbour tilt.

Fig. 5–7 show top views of the monolayer both adsorbed on the surface [Fig. 5(a), 6(a), 7(a) and 8) and in free space [Fig. 5(b), 6(b) and 7(b)]. These figures emphasize the change in the tilt direction on adsorption. The reorientation on adsorption is caused by the reorientation of the head groups to form hydrogen bonds with the surface carbonate ions. In general, anchoring the monolayer on the surface increases the order (reduces the entropy).

Conclusions

We have modelled the interfaces between the low index faces of calcite and monolayers of octadecanoic acid and found all interfaces considered to be strongly bound, with interfacial energies of around -1 J m^{-2}. The highest interfacial energy was found for the (001) Ca-terminated interface. The interfacial energy is one component required for the prediction of the relative nucleation rates for the various crystal faces on organic monolayers. As we found similar interfacial energies for all the interfaces considered, and the other components are as yet unknown, we cannot make any concrete predictions for the preferred nucleation face from the current simulations. Work is currently in progress to do this. Nevertheless, the high interfacial energies indicate that the monolayer strongly enhances the nucleation rate.

The adsorbed monolayers were found to have a significant effect on the relaxed surface crystal structures for some interfaces and the adsorption onto the surface also modified the configuration of the monolayer. The adsorbed monolayers had a more ordered conformation than the free monolayers and the alkane tail tilt directions were generally different due to the reorientation of the head groups at the surface.

An obvious issue is the effect of pH. The pK_a of octadecanoic acid is 5.6. The experiments of ref. 2 are performed using supersaturated solutions of calcium bicarbonate, which typically have a pH of 5.8–6.0. Using standard bulk solution arguments, one would therefore expect about 60% of the carbonyl groups to be ionised. This is probably an overestimate, since it ignores surface effects. We are currently performing calculations on the effect of pH and will report them in a future paper.

The simulations reported here have demonstrated that there is a strong interaction between the surfaces of calcite and monolayers of octadecanoic acid. Such monolayers will, therefore, substantially enhance the nucleation rate of calcite crystals from solution. However, the simple epitaxial matching arguments used in the literature are not sufficient. They suggest the kinds of geometrical arrangements that *could* enhance calcite growth; however, they cannot demonstrate which arrangements *will* do this because they are unable to predict the relative stabilities of different interfaces. Moreover, our results show that the monolayers alter the relaxed configuration of some surfaces significantly in several cases. This is particularly true for polar interfaces. In this case, we need to move beyond simple epitaxial arguments based on perfect lattices. We will address this point in a future publication.

Acknowledgements

We thank EPSRC for financial support under Grant No. GR/R25484 and Prof. S. C. Parker (University of Bath, UK) for helpful discussions.

References

1 L. T. Kuhn, D. J. Fink and A. H. Heuer, in *Biomimetic Materials Chemistry*, ed. S. Mann, VCH, New York, 1996, ch. 2, p.40.
2 (*a*) S. Mann, B. R. Heywood, S. Rajam and J. B. A. Walker, *J. Phys. D*, 1991, **24**, 11; (*b*) J. B. A. Walker, B. R. Heywood and S. Mann, *J. Mater. Chem.*, 1991, **1**, 889; (*c*) B. R. Heywood and S. Mann, *Chem. Mater.*, 1994, **6**, 311.
3 (*a*) J. Küther and W. Tremel, *Chem. Commun.*, 1997, 2029; (*b*) J. Küther, R. Seshadri, W. Knoll and W. Tremel, *J. Mater. Chem.*, 1998, **8**, 641; (*c*) J. Küther, R. Seshadri, G. Nelles, W. Assenmacher, H. J. Butt, W. Mader and W. Tremel, *Chem. Mater.*, 1999, **11**, 1317.
4 J. Aizenberg, A. J. Black and G. M. Whitesides, *Nature*, 1999, **398**, 495.
5 S. D. Sims, J. M. Didymus and S. Mann, *J. Chem. Soc., Chem. Commun.*, 1995, **10**, 1031.
6 N. Ueyama, T. Hosoi, Y. Yamada, M. Doi, T. Okamura and A. Nakamura, *Macromolecules*, 1998, **31**, 7119.
7 A. Berman and D. Charych, *J. Cryst. Growth*, 1999, **198/199**, 796.
8 W. Smith and T. R. Forester, *J. Mol. Graphics*, 1996, **14**, 136.
9 A. D. MacKerell Jr., D. Bashford, M. Bellott, R. L. Dunbrack Jr., J. D. Evanseck, M. J. Field, S. Fischer, J. Gao, H. Guo, S. Ha, D. Joseph-McCarthy, L. Kuchnir, K. Kuczera, F. T. K. Lau, C. Mattos, S. Michnick, T. Ngo, D. T. Nguyen, B. Prodhom, W. E. Reiher III, B. Roux, M. Schlenkrich, J. C. Smith, R. Stote, J. Straub, M. Watanabe, J. Wiórkiewicz-Kuczera, D. Yin and M. Karplus, *J. Phys. Chem. B*, 1998, **102**, 3586.
10 M. A. Moller, D. J. Tildesley, K. S. Kim and N. Quirke, *J. Chem. Phys.*, 1991, **94**, 8390.
11 A. Pavese, M. Catti, S. C. Parker and A. Wall, *Phys. Chem. Miner.*, 1996, **23**, 89.
12 N. L. de. Leeuw and S. C. Parker, *J. Phys. Chem. B*, 1998, **102**, 2914.
13 D. E. Parry, *Surf. Sci.*, 1975, **49**, 433; 1976, **54**, 195.
14 G. W. Watson, E. T. Kelsey, N. H. de. Leeuw, D. J. Harris and S. C. Parker, *J. Chem. Soc., Faraday Trans.*, 1996, **92**, 433.
15 J. H. Harding, *Surf. Sci.*, 1999, **422**, 87.
16 V. M. Kaganer, H. Mohwald and P. Dutta, *Rev. Mod. Phys.*, 1999, **71**, 779.